

RESEARCH PAPER

Electrospun PCL/chitosan nanofibrous scaffold for human bladder smooth muscle regeneration

Mohammad Ali Derakhshan¹, Ali Akbar Karimi Zarchi^{2*}, Parisa Ghadiri Harati³

¹Department of Medical Nanotechnology, School of Advanced Sciences and Technologies in Medicine, Shiraz University of Medical Sciences, Shiraz, Iran

²Nanobiotechnology Research Center, Baqiyatallah University of Medical Sciences, Tehran, Iran

³Department of Physiotherapy, School of Rehabilitation, Shahid Beheshti University of Medical Sciences, Tehran, Iran

ABSTRACT

Objective(s): Several pathologic complications may lead to defects in urinary bladder tissue or organ loss. In this regard, bladder tissue engineering utilizing electrospun nanofibrous PCL and PCL/chitosan would be promising as replacing structures.

Materials and Methods: The resultant nanofibers were characterized for their morphology, diameter and composition by scanning electron microscopy (SEM), and also, FT-IR and CHN analyses. Then, isolation of smooth muscle cells of human urinary bladder biopsies was performed and the obtained cells were characterized by immunocytochemistry (ICC). Thereafter, seeded cells on PCL and PCL/CS nanofibers were assayed for their viability/toxicity, and also, cell-scaffold attachments and cell morphologies were investigated.

Results: The findings illustrated that PCL and PCL/CS nanofibers of about 100 nm were successfully fabricated. The obtained scaffolds provided appropriate environment for attachment and expansion of seeded detrusor smooth muscle cells. Biocompatibility of both scaffolds was demonstrated by alamar blue assay. After 7 days of study, cells showed higher viability percentage on PCL/CS nanofibers.

Conclusion: Nanofibrous PCL or PCL/CS scaffolds could properly help adhesion and proliferation/growth of human bladder smooth muscle cells (hBSMCs).

Keywords: Bladder; Electrospun nanofiber; PCL; PCL/CS; Tissue engineering

How to cite this article

Derakhshan MA, Karimi Zarchi AA, Ghadiri Harati P. Electrospun PCL/chitosan nanofibrous scaffold for human bladder smooth muscle regeneration. *Nanomed J.* 2022; 9(2): 138-146. DOI: [10.22038/NMJ.2022.62927.1658](https://doi.org/10.22038/NMJ.2022.62927.1658)

INTRODUCTION

The function of urinary bladder as an important part of renal system may be disordered by some pathologic conditions. Indeed, bladder cancer, congenital abnormalities such as myelomeningocele and bladder exstrophy, inflammatory diseases and trauma may lead to severe bladder tissue defects or organ failure [1, 2]. Annually, around 150,000 patients die of bladder cancer and therefore, many patients need cystectomy [3]. In such complications, patients may be the candidates for bladder organ/tissue replacements.

The clinical operation to replace or augment the

damaged or removed bladder includes utilizing gastrointestinal segments (gastrocystoplasty) or other kinds of cystoplasties [4]. However, utilization of those non-native tissues increases the chance of metabolic disorders and other complications [5-8]. In these regards, novel replacing strategies for urinary bladder is required.

Bladder tissue engineering is introduced as a strategy to generate substitutes for native bladder tissue. In this respect, designing appropriate scaffolds providing biophysical and biochemical cues are needed. A variety of biological, synthetic or combined scaffolds have been reported with potential capabilities in tissue engineering [9-13]. In bladder tissue regeneration, although, different acellular tissue matrices [14-16] have been previously used to prepare bladder scaffolds, however, these structures suffer from

* Corresponding author: Email: a_karimi@bmsu.ac.ir

Note. This manuscript was submitted on January 2, 2022; approved on Mar 7, 2022

weak mechanical properties. Application of pure synthetic polymers or blended with biopolymers such as collagen, as a main protein of extra cellular matrix would be an alternative. In a breakthrough, *Atala et al.* reported notable results of their special collagen-poly glycolic acid structure applied for bladder reconstruction after cystectomy. Therefore, scaffolds made of different synthetic polymers have been utilized in supporting urothelial cells and bladder smooth muscle [17-19]. These scaffolds could be processed by a variety of techniques [20].

Electrospinning has been vastly utilized as a convenient and flexible approach to prepare scaffolds of various fiber diameters, morphologies and geometries [21-23]. The resultant fibrous scaffolds would resemble the natural extracellular matrix (ECM) by providing the bio-physical and biochemical cues in a network of fibers with special topographies, chemical composition and mechanical characteristics that support cell functions [24, 25]. In this respect, electrospun fibers of synthetic/natural polymer sources such as poly L-lactic acid (PLLA) [26], PVDF/collagen [27], fibrinogen [28], silk fibroin [29], PLGA [30, 31], poly-acrylonitrile/polyethylene oxide (PAN/PEO) [32] and core/shell PLCL/Hyaluronic acid [33] have been utilized in bladder tissue regeneration.

Poly(ϵ -caprolactone) (PCL), as a synthetic polymer, is frequently utilized in fabricating electrospun nanofibers for tissue regeneration regarding its notable mechanical strength, biocompatibility and biodegradability [34, 35]. Therefore, in some studies, nanofibrous scaffolds containing PCL have been used for bladder tissue engineering [36-38]. However, to provide more appropriate interactions of cell-scaffold, bio-functional groups have been rendered to the synthetic PCL by its blending with biopolymers such as chitosan (CS) [39, 40]. Chitosan as a polysaccharide, containing monomers of glucose amine and N-acetyl glucose amine, is hydrophilic and biocompatible. Also, antibacterial, fungi-static and hemo-static properties of this natural polymer are reported [40-43]. Furthermore, in tissue engineering applications, it could render chemical cues for cell binding and other functions due to its resemblance to ECM glycosaminoglycans (GAGs) [44].

In the present study, the bio-compatibility and interactions of human bladder smooth muscle cells (hBSMCs) with electrospun nanofibers (mean diameters around 100 nm), with/without bio-functional surface groups, were investigated.

As mentioned before, the morphology of the prepared structures along with biochemical cues would affect cell functions including cellular attachment, expansion and proliferation. In this regard, electrospun PCL and PCL/CS fibers were fabricated through electrospinning and their capability in supporting smooth muscle cells of detrusor was investigated. Properties of nanofibers were analysed with scanning electron microscopy (SEM), FT-IR and CHN analyses. Then, isolation of smooth muscle cells of urinary bladder specimens was performed and the obtained cells were identified by immunocytochemistry (ICC). Thereafter, cell-seeding was done on PCL and PCL/CS nanofibers to evaluate the biocompatibility of the scaffolds, cell-scaffold attachments and cell morphologies.

MATERIALS AND METHODS

Materials

PCL polymer (70 kDa) was received from Hangzhou Ruijiang Chemical Co., Ltd, China. Low molecular weight chitosan (CS, deacetylation degree: 91.2 %) was purchased from Easter Group (Dong Chen) Co. Ltd, China. Chloroform, methanol, Formic acid, acetic acid, and acetone were obtained from Merck Co., Germany. Lab-scale electrospinning set was purchased from Fanavaran Nano-Meghyas Co. Ltd, Tehran, Iran.

Preparation of nanofibrous scaffolds

For electrospinning of PCL, 4-10.0 wt. % polymer solutions were prepared in chloroform/methanol solvent [4:1, v/v] and also, separately, 9.0 wt. % in formic acid/acetic acid [1:1, v/v]. Then, to electrospun blended solutions of PCL and CS, a previously reported method [45] was used with some modifications. First, PCL polymer was dissolved in formic acid/acetone [4/1, v/v] at concentration of 12.0 wt. %. Chitosan solution (2.0 wt. %) was prepared in formic acid. A blend solution of PCL/chitosan was provided with a weight ratio of 8/2, v/v. Thereafter, for each process, the polymeric solution was loaded in a 5 ml plastic syringe having a 23G needle. Then, electrospinning was done under a solution flow rate of 0.5-1 ml.h⁻¹, collector-tip distance of 100 mm, high voltage 20 kV and collector rotation of 200 rpm. The resultant nanofibrous scaffolds were deposited on an aluminium foil.

Characterization of the nanofibers

Scanning electron microscopy (SEM)

To evaluate the diameter of the obtained

nanofibers and observe surface morphologies, SEM (XL 30, Philips, USA, 25.0 kV) was used. Prior to observation, gold sputter-coating was done on each sample and then, related micro-graphs were recorded. Thereafter, specimen images were analysed by imageJ (imagj.nih.gov/ij) to measure the mean size of about 100 nanofibers.

Fourier-transform infrared (FT-IR) spectroscopy

To confirm the existence of CS and PCL in the blend PCL/CS electrospun samples, compositional evaluation of each polymer and also, the blended PCL/CS specimens were carried out separately by using a FTIR spectrometer (Equinox 55, Bruker, Germany, range: 4000-500 cm^{-1} , resolution: 4 cm^{-1}).

CHN analysis

The content of hydrogen (H), nitrogen (N) and carbon (C) elements of the nanofibers were analyzed by an elemental analyzer.

Bladder smooth muscle cell isolation

After providing written consents and ethical considerations, bladder specimens (around 1cm³) of patients under anti-reflux or prostatectomy surgical operations were received. Based on our previous report [26], the specimens were sterilized, the urothelium was discarded and smooth muscle of detrusor was cut into small pieces. Thereafter, partial enzymatic digestion of the sample was done using collagenase type IV for 1 hour (37°C). Afterwards, the enzyme was eliminated by centrifugation and the obtained cells were cultured and expanded in complete media having Dulbecco's Modified Eagles Medium (DMEM), containing 20% fetal bovine serum (FBS) and 1% penicillin/streptomycin. Then, the culture flasks were incubated in a humidified atmosphere containing 5% CO₂ at 37°C.

Immunocytochemistry

To characterize the isolated cells for their specific biomarkers, immunocytochemistry against actin by mouse anti- α -SMA (Abcam) was done. The isolated hBSMCs cultured in plates were washed with PBS and then, fixed with paraformaldehyde (4%) 12 min at room temperature (RT). Thereafter, the cells were washed with PBS having Tween-20 (0.05%, TPBS) and permeabilization was done using Triton X-100 (0.2 %). After three-time rinsing the cells with TPBS, blocking was performed using 1% BSA in TPBS (1 h, RT). Then, hBSMCs were incubated with primary antibody (anti- α -SMA, 1:50) overnight (4°C). Subsequently, the cells

were rinsed with TPBS and treated with secondary anti-mouse antibody (1:250), 1 h at RT (in dark). Then, cells were rinsed with PBS, and fluorescence microscopy was used to observe the cells.

Cell study on electrospun nanofibers

To evaluate the interactions of hBSMCs with the prepared nanofibers, cultured cells were trypsinized and seeded on the PCL and PCL/CS scaffolds. In this respect, circular electrospun samples (around 7 mm) were sterilised with 70% ethanol and irradiated with UV (20 min.). Thereafter, cell-seeding on PCL/CS and PCL nanofiber circular samples was done using 1×10⁵ cells in DMEM complete media, containing 20% FBS and 1% pen/strep. Finally, the test plates were kept in an incubator (37°C, 5% CO₂).

To investigate cell morphologies on the PCL/CS and PCL fibers after 2 days, SEM microscopy was utilized. First, the specimens were washed with PBS, and fixing with 2.5% paraformaldehyde plus 2% glutaraldehyde (1 h, at 4°C) was performed. Thereafter, an increasing serial concentration of ethanol was used for sample dehydration. Finally, and after air drying of the samples, gold sputter-coating was done on each specimen, before observing by SEM (25.0 kV).

Viability of cells on nanofibrous scaffolds

To evaluate and quantify the viability and proliferation rate of seeded cells, alamar blue assay was used. This assay shows no interruption or toxicity on the cell activities under culture, therefore, allows for a continuous cell study on nanofibers. In this regard, the medium on each sample was aspirated carefully at pre-set time points and thereafter, 100 μ l of complete media containing 10% alamar blue solution (1mg/ml) was replaced and kept in an incubator for further 3 h. For negative and positive controls, wells having assay solution lack of cells and wells containing cells in media-dye without scaffold were utilized, respectively. Finally, the absorbance of reduced form of dye in wells was measured at 570 and 600 nm. The studies were done in triplicate and results were reported as means \pm SD.

The following equation was used for calculations:

$$\text{Cell Proliferation (\%)} = \frac{[(\epsilon\text{OX})\lambda_1 \cdot A\lambda_1 - (\epsilon\text{OX})\lambda_1 \cdot A\lambda_2 / (\epsilon\text{OX})\lambda_2 \cdot A'\lambda_1 - (\epsilon\text{OX})\lambda_1 \cdot A'\lambda_2]}{\times 100}$$

Here, $A\lambda_1$ and $A\lambda_2$ are the absorbance values for sample wells read at the wavelengths $\lambda_1 = 570$ nm and $\lambda_2 = 600$ nm. $A'\lambda_1$ and $A'\lambda_2$ represent the

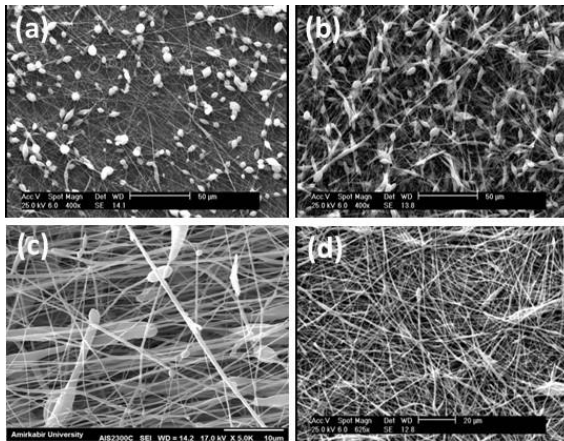


Fig. 1. SEM micrographs of electrospun PCL nanofibers with concentrations of 6% (a), 8% (b), 9% (c) and 10% w/w (d) in chloroform/methanol mixed solvents

absorbance measured for positive control. Also, the molar extinction coefficients for oxidized alamar blue ($\epsilon_{OX}(\lambda_1) = 80.586$ and $\epsilon_{OX}(\lambda_2) = 117.216$) were used in the formula.

RESULTS AND DISCUSSION

Diameter and morphology of nanofibers

To prepare electrospun nanofibers of PCL, different solvents were utilized. Application of a chloroform/methanol (4/1, v/v) mixture resulted in the formation of smooth nanofibers in 10% wt. PCL solution (Fig. 1). According to Fig. 1, augmenting the concentration of polymer from 6% to 10% wt. could result in bead-free and smooth fibers. It is known that augmenting the polymer concentration would provide more polymer entanglements and production of continuous nanofibers [46]. Electrospinning of the 10% wt. solution led to the nanofibers of 260 ± 103 nm in diameter. As it is hard to fabricate electrospun PCL fibers of smaller diameters in chloroform/methanol mixture, in the next step, a formic/acetic acid (1:1, v/v) solvent system was utilized. As shown in Fig. 2, electrospinning of the 9% wt. PCL solution in such acidic solvent could form defect-free 118 ± 15 nm fibers with a narrow dispersion of diameters (Fig. 2c). The reduction in fiber size when using acidic solvent could be attributed to the high conductivity of formic acid ($157.5 \mu\text{S}/\text{cm}$) compared to that of chloroform/methanol ($0.5 \mu\text{S}/\text{cm}$). Indeed, an increased electrical conductivity would result in a higher surface charge on the polymeric jet. Consequently, electrospinning

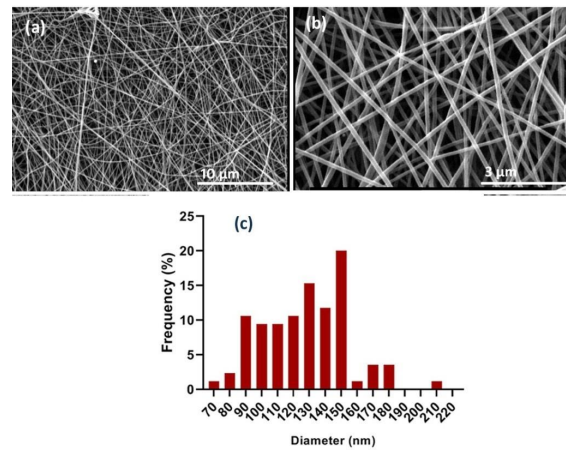


Fig. 2. The SEM micrographs of PCL nanofibers with concentration of 9%, wt. (a, b), in formic/acetic acid mixed solvent, and chart of nanofiber diameter distribution (c)

solution experiences a raised extension due to huge electric charge repulsions that resulted in the formation of thinner fibers [47].

Electrospinning of a blend solution of PCL/CS polymers was followed using formic acid and acetone solvents. It has been previously reported that a combination of these two solvents helps preparation of non-woven PCL/CS nanofibers through electrospinning [45]. Optimization of the process to provide appropriate sizes and morphologies of nanofibers was followed by controlling parameters; i.e. polymeric solution concentrations, blending weight ratios, solution feeding rate, working distance and applied voltage. Thereafter, the produced nanofibers were characterized by SEM. Fig. 3(a, b) depicts the micrographs of the resultant PCL/CS nanofibers and the corresponding size distribution chart. As it is shown, the nanofibers illustrate random orientations with defect-free smooth morphologies. Also, diameter distribution chart of the obtained fibers is represented in Fig. 3c, respectively. The mean diameter of PCL/CS nanofibers is 92 ± 31 nm. Chitosan biopolymer in acidic solution is highly protonated that imposes an increased extension on the electrospinning jet due to the positive charge repulsions and therefore, results in finer fibers [48]. It is in line with other studies reporting a reduction of fiber diameters in electrospun PCL/CS nanofibers [49, 50]. According to our previous report, small diameter nanofibers provide more attachment sites for cellular binding proteins, therefore help appropriate expansion of

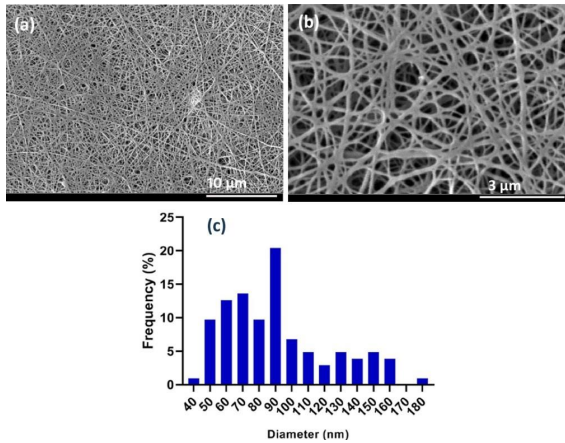


Fig. 3. SEM images of electrospun PCL/CS (blend ratio of 8/2, v/v) nanofibers (a, b), in formic/acetone mixed solvent, and chart of nanofiber diameter distribution (c)

the cells on the scaffolds [26]. Accordingly, it would be expected that smooth muscle cells find their elongated morphology on the obtained fibers.

FT-IR analyses

To analyse the composition of the prepared scaffolds and to confirm the presence of chitosan in blended samples, FTIR spectroscopy was performed. The spectra of FT-IR analyses of PCL and PCL/CS nanofibers specimens and also, neat CS polymer are shown in the Fig. 4. For CS sample, the band at 3387 cm^{-1} shows the stretching of N-H and O-H [40]. Also, absorptions at 1032 and 1072 cm^{-1} could be assigned to the stretches of C-O and the peak at 1154 cm^{-1} illustrates the C-O-C asymmetric stretches. The characteristic bands at 1380 and 1428 cm^{-1} could be due to the symmetrical deformation of CH₃ and bending of CH₂, respectively [51-53]. The peaks at 1600 , 1330 and 1658 cm^{-1} correspond to the bending of N-H (in primary amine), and stretching of C-N (amide III) and C=O (amide I), respectively [53, 54]. Also, the bands at 2894 and 2941 cm^{-1} could be the asymmetrical and symmetrical stretches of C-H [53]. FTIR analysis of PCL polymer illustrated C=O stretching vibrations at 1725 cm^{-1} . Also, stretching vibration of CH₂ was located at 2869 and 2951 cm^{-1} [55]. According to the characteristic peaks of chitosan and PCL, absorption bands of N-H and O-H (around 3430 cm^{-1}), stretching vibration of CH₂ (2861 and 2925 cm^{-1}), C=O stretching vibrations (1722 cm^{-1}) could be detected in PCL/CS nanofibers (Fig. 4).

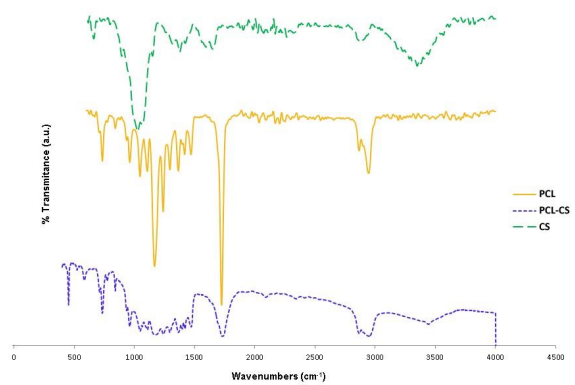


Fig. 4. FT-IR spectra of PCL, CS and PCL/CS samples

CHN analyses

According to the Fig. 5, CHN analyses illustrated the existence of nitrogen only in the PCL/CS nanofiber specimen, compared to the PCL sample that showed only peaks of carbon and hydrogen elements. It demonstrates that chitosan is incorporated in the blended samples.

Cell isolation and identification

Fig. 6a-b shows the optical microscopy images of hBSMCs on tissue culture plate. It is clear that the isolated cells have found their characteristic elongated shape. Indeed, these cells were migrated efficiently from small pieces of partially digested bladder muscle tissue. Further, ICC was done for

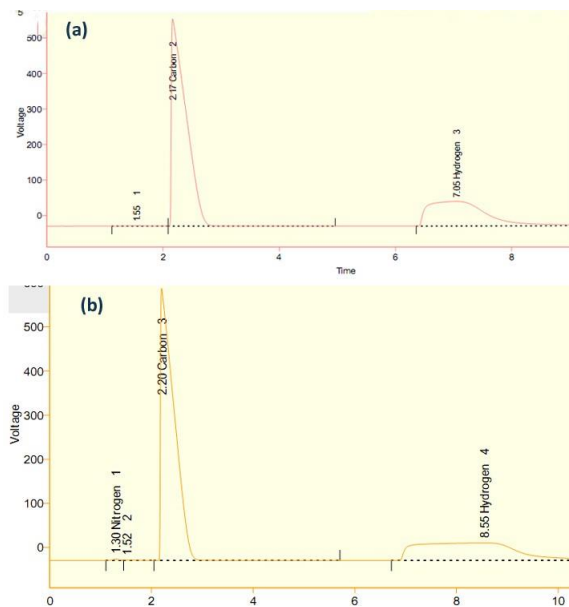


Fig. 5. peaks of CHN analyses for PCL (a) and PCL/CS nanofibers (b)

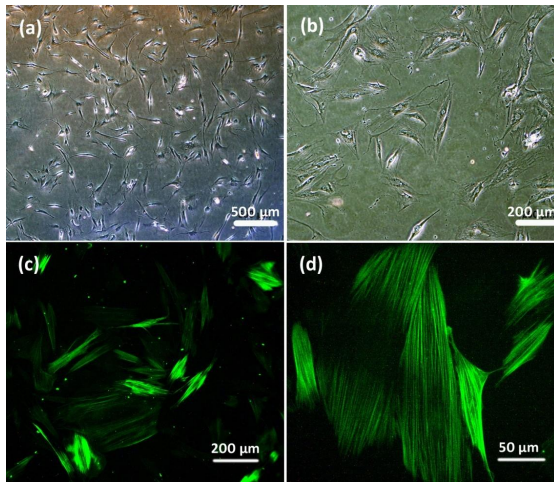


Fig. 6. The hBSMCs on TCP (a, b), and immuno-staining of the isolated hBSMCs against alpha-SMA (c, d)

phenotypic identification of the isolated cells. Fig. 6c-d depict immuno-stained cells against smooth muscle marker (α -SMA). The images illustrate that strong expression of α -actin has elongated the cells along the axis of filaments.

Cell-nanofiber interactions and compatibility

Fig. 7 represents the results of the alamar blue assay for cell viability in a 7-day evaluation. Accordingly, human bladder smooth muscle cells have shown proper viability on both PCL and PCL/CS electrospun samples. Indeed, no significant statistical difference between test samples and control was observed. Therefore, PCL/CS nanofibrous scaffolds would be considered as a cyto-compatible cell seeding support. However, an increased mean viability of smooth muscle cells on PCL/CS nanofibers after 1 week of seeding is clear according to the Fig. 7,b.

According to the previous studies, different cellular activities, i.e. cell viability and proliferation, finding natural morphology and differentiation, would be controlled by designing nanofibrous scaffolds of various fiber physicochemical properties [25, 56-58]. In this respect, controlling nanofiber diameter, morphology, chemical composition and some other items could help interactions of cells and nanofibers to begin cell adhesion/spreading on the nanofibers surface [20, 24]. Differentiated bladder smooth muscle cells show an elongated morphology and make bundles in their natural tissue [59].

Previously, capabilities of the PCL electrospun

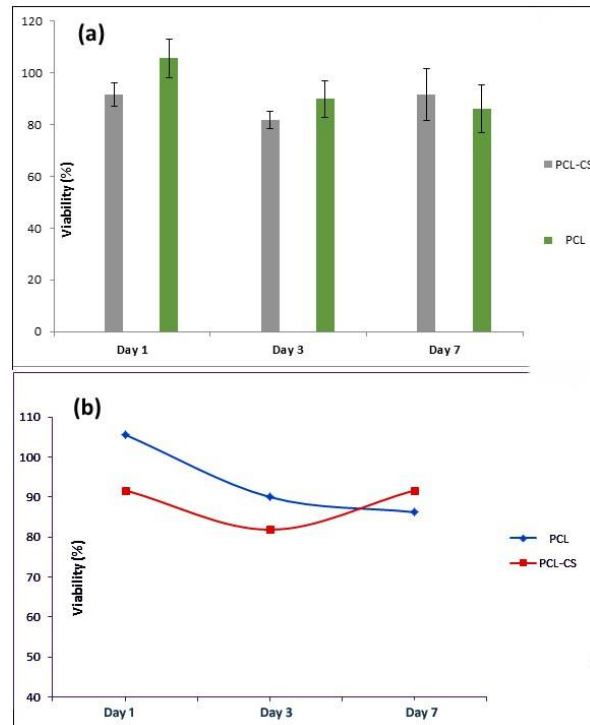


Fig. 7. Charts of alamar blue assay results for cell viability percentages on PCL and PCL/CS electrospun scaffolds

nanofibers in supporting urinary bladder smooth muscle cells have been shown [38, 60]. However, PCL as a synthetic polymer possess hydrophobic properties lack of special cell binding functional groups [61, 62]. Therefore, blending PCL polymer with natural polymers would result in improving hydrophilicity of the obtained nanofibers [63, 64]. In a study, smooth muscle cells seeded on the PCL nanofibers showed poor growth and coating of the fibers with collagen improved cell adhesion and growth significantly [65]. Indeed, utilizing biopolymers in association with synthetic ones would render cell interaction sites to the electrospun scaffolds. In this regard, PCL/CS nanofibers have been prepared for various tissue regeneration aims [39, 50, 66]. Recently, Zhou *et al.* have demonstrated the capability of freeze-dried compression molded PCL/CS scaffolds in bladder tissue engineering [67]. They reported the successful differentiation of adipose-derived stem cells to bladder smooth muscle cells on scaffolds and an enlargement in bladder capacity and angiogenesis was observed *in vivo*. Also, the authors reported that compared to appropriate regeneration of urothelium layers, smooth muscle

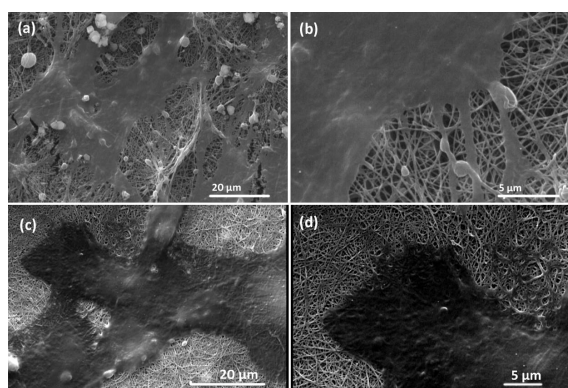


Fig. 8. SEM micrographs of the hBSMCs on the PCL (a, b), and PCL/CS (c, d) scaffolds after 48h of seeding; scale bars: 20 μm (a, c) and 5 μm (b, d)

cells illustrated sparser on the PCL graft. Therefore, preparing PCL/CS electrospun nanofibers would provide proper conditions for bladder smooth muscle cells to attach and perform their functions.

According to the Fig. 8, hBSMCs seeded on PCL or PCL/CS nanofiber scaffolds for 48 h are attached in numerous points, i.e. focal adhesions, to the fibers and are completely expanded. As it is clear, the cells show casual morphologies and no elongation besides each other is observable. Also, due to the very fine diameter of both PCL and PCL/CS nanofibers and their narrow size distribution, and huge size of smooth muscle cells, no infiltration to the scaffold could be detected. The seeded bladder smooth muscle cells could be elongated to more than 100 μm . The previous studies on the morphology of the isolated hBSMCs on electrospun random PCL/PLLA [36] and PLLA [26] nanofibers demonstrated that in the early days of cell seeding, they show random morphologies. However, after 1 month of seeding, the cells are totally elongated and oriented along each other on the randomly-arranged electrospun nanofibers [26]. It suggests that random PCL and PCL/CS electrospun nanofibers could provide appropriate scaffold for bladder detrusor tissue engineering. However, investigation of mechanical characteristics of the prepared bladder scaffolds needs to be considered in the future studies, according to its important role in the regeneration process [68, 69].

CONCLUSION

In the present study, random electrospun PCL and PCL/CS nanofibers were successfully prepared and characterized utilizing SEM, FT-IR and CHN

analyses. In the resultant nanofibers, addition of chitosan solution to the PCL acidic solution could reduce fiber diameters. Both prepared polymeric scaffolds showed compact fibers of smooth morphology and around 100 nm in diameter. Then, isolated- smooth muscle cells were identified by ICC against their α -actin expression. The seeded cells on the scaffolds illustrated appropriate attachment due to numerous focal adhesions and showed casual cell morphologies on the scaffolds. Also, the results of cytotoxicity assays demonstrated the biocompatibility of obtained scaffolds with hBSMCs. In this regard, it could be concluded that random electrospun PCL and PCL/CS nanofibrous scaffolds would provide proper environment for bladder tissue engineering.

ACKNOWLEDGMENTS

The authors gratefully thank Baqiatallah University of Medical Sciences for supporting the present research.

STATEMENT OF ETHICS

The research is followed under the ethical approval of Baqiatallah University of Medical Sciences (Ethical code: IR.BMSU.REC.1397.038).

CONFLICT OF INTEREST

The authors declare that there is no conflict of interest.

REFERENCES

- Atala A. Tissue engineering of human bladder. *British medical bulletin*. 2011;97(1):81-104.
- Kumar N, Saxena S, Kumar V, Shrivastava S, Gangwar AK, Maiti SK, et al. Scaffolds for bladder tissue engineering. *Handbook of Tissue Engineering Scaffolds: Volume Two*: Elsevier; 2019. p. 493-548.
- Siegel R, Ward E, Brawley O, Jemal A. Cancer statistics, 2011. *CA Cancer J Clin*. 2011;61(4):212-236.
- Petrovic V, Stankovic J, Stefanovic V. Tissue engineering of the urinary bladder: current concepts and future perspectives. *ScientificWorldJournal*. 2011;11:1479-1488.
- McDougal WS. Metabolic complications of urinary intestinal diversion. *J Urol*. 1992;147:1199-208.
- KAEFER M, HENDREN WH, BAUER SB, GOLDENBLATT P, PETERS CA, ATALA A, et al. Reservoir calculi: a comparison of reservoirs constructed from stomach and other enteric segments. *J Urol*. 1998;160(6):2187-2190.
- Kaefer M, Tobin MS, Hendren WH, Bauer SB, Peters CA, Atala A, et al. Continent urinary diversion: the Children's Hospital experience. *J Urol*. 1997;157(4):1394-1399.
- Filmer RB, Spencer JR. Malignancies in bladder augmentations and intestinal conduits. *J Urol*. 1990;143(4):671-678.
- Dehqan Niri A, Karimi Zarchi AA, Ghadiri Harati P, Salimi A, Mujokoro B. Tissue engineering scaffolds in the treatment

- of brain disorders in geriatric patients. *Artificial Organs*. 2019;43(10):947-960.
10. Firoozi S, Amani A, Derakhshan MA, Ghanbari H, editors. Artificial Neural Networks modeling of electrospun polyurethane nanofibers from chloroform/methanol solution. *J Nano Res*. 2016: Trans Tech Publ.
 11. Babaloo H, Ebrahimi-Barough S, Derakhshan MA, Yazdankhah M, Lotfibakhshaiesh N, Soleimani M, et al. PCL/gelatin nanofibrous scaffolds with human endometrial stem cells/Schwann cells facilitate axon regeneration in spinal cord injury. *J Cell Physiol*. 2019;234(7):11060-11069.
 12. Shahrusvand M, Ghollasi M, Zarchi AAK, Salimi A. Osteogenic differentiation of hMSCs on semi-interpenetrating polymer networks of polyurethane/poly(2-hydroxyethyl methacrylate)/cellulose nanowhisker scaffolds. *Int J Biol Macromol*. 2019;138:262-271.
 13. Ahmadi P, Nazeri N, Derakhshan MA, Ghanbari H. Preparation and characterization of polyurethane/chitosan/CNT nanofibrous scaffold for cardiac tissue engineering. *Int J Biol Macromol*. 2021.
 14. Kajbafzadeh A-M, Payabvash S, Salmasi AH, Sadeghi Z, Elmi A, Vejdani K, et al. Time-dependent neovascularization and regeneration of different bladder wall components in the bladder acellular matrix graft in rats. *J of Surg Res*. 2007;139(2):189-202.
 15. Zhang Y, Kropp BP, Moore P, Cowan R, FURNESS PD, KOLLIGIAN ME, et al. Coculture of bladder urothelial and smooth muscle cells on small intestinal submucosa: potential applications for tissue engineering technology. *J Urol*. 2000;164(3):928-935.
 16. Zhang Y, Frimberger D, Cheng EY, Lin Hk, Kropp BP. Challenges in a larger bladder replacement with cell-seeded and unseeded small intestinal submucosa grafts in a subtotal cystectomy model. *BJU int*. 2006;98(5):1100-1105.
 17. Atala A, Vacanti J, Peters C, Mandell J, Retik A, Freeman M. Formation of urothelial structures in vivo from dissociated cells attached to biodegradable polymer scaffolds in vitro. *J Urol*. 1992;148(2 Pt 2):658-662.
 18. Hoque ME, San WY, Wei F, Li S, Huang M-H, Vert M, et al. Processing of polycaprolactone and polycaprolactone-based copolymers into 3D scaffolds, and their cellular responses. *Tissue Eng Part A*. 2009;15(10):3013-3024.
 19. Xu F, Wang Y, Jiang X, Tan H, Li H, Wang K-J. Effects of different biomaterials: Comparing the bladder smooth muscle cells on waterborne polyurethane or polylactic-co-glycolic acid membranes. *Kaohsiung J Med Sci*. 2012;28(1):10-15.
 20. Beachley V, Wen X. Polymer nanofibrous structures: Fabrication, biofunctionalization, and cell interactions. *Prog Polym Sci*. 2010;35(7):868-892.
 21. Sun B, Long YZ, Zhang HD, Li MM, Duvail JL, Jiang XY, et al. Advances in three-dimensional nanofibrous macrostructures via electrospinning. *Prog Polym Sci*. 2014;39(5):862-890.
 22. Arvand M, Mirzaei E, Derakhshan MA, Kharrazi S, Sadroddiny E, Babapour M, et al. Fabrication of antibacterial silver nanoparticle-modified chitosan fibers using Eucalyptus extract as a reducing agent. *J Appl Polym Sci*. 2015;132(25).
 23. Wei G, Li C, Fu Q, Xu Y, Li H. Preparation of PCL/silk fibroin/collagen electrospun fiber for urethral reconstruction. *Int Urol Nephrol*. 2015;47(1):95-99.
 24. Oguer KS, Laurencin CT. Nanofiber Technology for Regenerative Engineering. *ACS Nano*. 2020;14(8):9347-9363.
 25. Li Y, Xiao Y, Liu C. The horizon of materiobiology: a perspective on material-guided cell behaviors and tissue engineering. *Chem Rev*. 2017;117(5):4376-421.
 26. Derakhshan MA, Pourmand G, Ai J, Ghanbari H, Dinarvand R, Naji M, et al. Electrospun PLLA nanofiber scaffolds for bladder smooth muscle reconstruction. *Int Urol Nephrol*. 2016;48(7):1097-1104.
 27. Mokhames Z, Rezaie Z, Ardeshiryajimi A, Basiri A, Taheri M, Omrani MD. VEGF-incorporated PVDF/collagen nanofibrous scaffold for bladder wall regeneration and angiogenesis. *Int J Polym Mater Polym Biomater*. 2020:1-9.
 28. McManus M, Boland E, Sell S, Bowen W, Koo H, Simpson D, et al. Electrospun nanofibre fibrinogen for urinary tract tissue reconstruction. *Biomed Mater*. 2007;2(4):257.
 29. Huang JW, Xu YM, Li ZB, Murphy SV, Zhao W, Liu QQ, et al. Tissue performance of bladder following stretched electrospun silk fibroin matrix and bladder acellular matrix implantation in a rabbit model. *J Biomed Mater Res Part A*. 2015.
 30. Sharifiaghdas F, Naji M, Sarhangnejad R, Rajabi-Zeleti S, Mirzadeh H, Zandi M, et al. Comparing Supportive Properties of Poly Lactic-Co-Glycolic Acid (PLGA), PLGA/Collagen and Human Amniotic Membrane for Human Urothelial and Smooth Muscle Cells Engineering. *Urol J*. 2014;11(3):1620-1628.
 31. Mirzaei A, Saburi E, Islami M, Ardeshiryajimi A, Omrani MD, Taheri M, et al. Bladder smooth muscle cell differentiation of the human induced pluripotent stem cells on electrospun Poly (lactide-co-glycolide) nanofibrous structure. *Gene*. 2019;694:26-32.
 32. Fakhrieh M, Darvish M, Ardeshiryajimi A, Taheri M, Omrani MD. Improved bladder smooth muscle cell differentiation of the mesenchymal stem cells when grown on electrospun polyacrylonitrile/polyethylene oxide nanofibrous scaffold. *J cell biochem*. 2019;120(9):15814-15822.
 33. Feng C, Liu C, Liu S, Wang Z, Yu K, Zeng X. Electrospun Nanofibers with Core-Shell Structure for Treatment of Bladder Regeneration. *Tissue Eng Part A*. 2019;25(17-18):1289-1299.
 34. Mochane MJ, Motsoeneng TS, Sadiku ER, Mokhena TC, Sefadi JS. Morphology and properties of electrospun PCL and its composites for medical applications: A mini review. *Appl Sci*. 2019;9(11):2205.
 35. Derakhshan MA, Nazeri N, Khoshnevisan K, Heshmat R, Omidfar K. Three-layered PCL-collagen nanofibers containing melilotus officinalis extract for diabetic ulcer healing in a rat model. *J Diabetes Metab Disord*. 2022:1-9.
 36. Shakhssalim N, Rasouli J, Moghadasali R, Aghdas FS, Naji M, Soleimani M. Bladder smooth muscle cells interaction and proliferation on PCL/PLLA electrospun nanofibrous scaffold. *Int J Artif Organs*. 2013;36(2):113-120.
 37. Ahvaz HH, Soleimani M, Mobasheri H, Bakhshandeh B, Shakhssalim N, Soudi S, et al. Effective combination of hydrostatic pressure and aligned nanofibrous scaffolds on human bladder smooth muscle cells: implication for bladder tissue engineering. *J Mater Sci Mater Med*. 2012;23(9):2281-2290.
 38. Costantino Del G, Alberto V, Guido B, Vincenza M, Angelo S, Alessandro Z, et al. Evaluation of electrospun bioresorbable scaffolds for tissue-engineered urinary bladder augmentation. *Biomed Mater*. 2013;8(4):045013.
 39. Semnani D, Naghashzargar E, Hadjianfar M, Dehghan Manshadi F, Mohammadi S, Karbasi S, et al. Evaluation of PCL/chitosan electrospun nanofibers for liver

- tissue engineering. *Int J Polym Mater Polym Biomater.* 2017;66(3):149-157.
40. Das P, Remigy J-C, Lahitte J-F, van der Meer AD, Garmy-Susini B, Coetsier C, et al. Development of double porous poly (ϵ -caprolactone)/chitosan polymer as tissue engineering scaffold. *Mater Sci Eng C.* 2020;107:110257.
 41. Hong S, Kim G. Fabrication of electrospun polycaprolactone biocomposites reinforced with chitosan for the proliferation of mesenchymal stem cells. *Carbohydr Polym.* 2011;83(2):940-946.
 42. Zhou X, Kong M, Cheng X, Li J, Li J, Chen X. Investigation of acetylated chitosan microspheres as potential chemoembolic agents. *Colloids Surf B: Biointerfaces.* 2014;123:387-394.
 43. Movaffagh J, Bazzaz F, Yazdi AT, Sajadi-Tabassi A, Azzadeh M, Najafi E, et al. Wound Healing and Antimicrobial Effects of Chitosan-hydrogel/Honey Compounds in a Rat Full-thickness Wound Model. *Wounds.* 2019;31(9):228-235.
 44. Costa-Pinto AR, Martins AM, Castelhana-Carlos MJ, Correlo VM, Sol PC, Longatto-Filho A, et al. In vitro degradation and in vivo biocompatibility of chitosan-poly (butylene succinate) fiber mesh scaffolds. *J Bioact Compat Polym.* 2014;29(2):137-151.
 45. Shalumon K, Anulekha K, Girish C, Prasanth R, Nair S, Jayakumar R. Single step electrospinning of chitosan/poly (caprolactone) nanofibers using formic acid/acetone solvent mixture. *Carbohydr Polym.* 2010;80(2):413-419.
 46. McKee MG, Wilkes GL, Colby RH, Long TE. Correlations of Solution Rheology with Electrospun Fiber Formation of Linear and Branched Polyesters. *Macromolecules.* 2004;37(5):1760-1767.
 47. Casasola R, Thomas NL, Trybala A, Georgiadou S. Electrospun poly lactic acid (PLA) fibres: Effect of different solvent systems on fibre morphology and diameter. *Polymer.* 2014;55(18):4728-4737.
 48. Najafi-Taher R, Derakhshan MA, Faridi-Majidi R, Amani A. Preparation of an ascorbic acid/PVA-chitosan electrospun mat: a core/shell transdermal delivery system. *RSC Adv.* 2015;5(62):50462-50469.
 49. Saderi N, Rajabi M, Akbari B, Firouzi M, Hassannejad Z. Fabrication and characterization of gold nanoparticle-doped electrospun PCL/chitosan nanofibrous scaffolds for nerve tissue engineering. *J Mater Sci Mater Med.* 2018;29(9):134.
 50. Mahoney C, Conklin D, Waterman J, Sankar J, Bhattarai N. Electrospun nanofibers of poly (ϵ -caprolactone)/depolymerized chitosan for respiratory tissue engineering applications. *J Biomater Sci Polym Ed.* 2016;27(7):611-625.
 51. Vino AB, Ramasamy P, Shanmugam V, Shanmugam A. Extraction, characterization and in vitro antioxidative potential of chitosan and sulfated chitosan from Cuttlebone of *Sepia aculeata* Orbigny, 1848. *Asian Pac J Trop Biomed.* 2012;2(1):S334-S341.
 52. Song C, Yu H, Zhang M, Yang Y, Zhang G. Physicochemical properties and antioxidant activity of chitosan from the blowfly *Chrysomya megacephala* larvae. *Int J Biol Macromol.* 2013;60:347-354.
 53. Fernandes Queiroz M, Melo KRT, Sabry DA, Sasaki GL, Rocha HAO. Does the use of chitosan contribute to oxalate kidney stone formation? *Marine drugs.* 2015;13(1):141-158.
 54. Lim S-H, Hudson SM. Synthesis and antimicrobial activity of a water-soluble chitosan derivative with a fiber-reactive group. *Carbohydr Res.* 2004;339(2):313-319.
 55. Yang S, Li X, Liu P, Zhang M, Wang C, Zhang B. Multifunctional Chitosan/Polycaprolactone Nanofiber Scaffolds with Varied Dual-Drug Release for Wound-Healing Applications. *ACS Biomater Sci Eng.* 2020;6(8):4666-4676.
 56. Shokraei S, Mirzaei E, Shokraei N, Derakhshan MA, Ghanbari H, Faridi-Majidi R. Fabrication and characterization of chitosan/kefiran electrospun nanofibers for tissue engineering applications. *J Appl Polym Sci.* 2021;138:e50547.
 57. Nazeri N, Derakhshan MA, Faridi-Majidi R, Ghanbari H. Novel electro-conductive nanocomposites based on electrospun PLGA/CNT for biomedical applications. *J Mater Sci Mater Med.* 2018;29(11):1-9.
 58. Firoozi S, Derakhshan MA, Karimi R, Rashti A, Negahdari B, Faridi Majidi R, et al. Fabrication and characterization of nanofibrous tricuspid valve scaffold based on polyurethane for heart valve tissue engineering. *Nanomater Res J.* 2017;2(2):131-141.
 59. Brown AL, Brook-Allred TT, Waddell JE, White J, Werkmeister JA, Ramshaw JA, et al. Bladder acellular matrix as a substrate for studying *in vitro* bladder smooth muscle-urothelial cell interactions. *Biomaterials.* 2005;26(5):529-543.
 60. Shakhssalim N, Dehghan MM, Moghadasali R, Soltani MH, Shabani I, Soleimani M. Bladder tissue engineering using biocompatible nanofibrous electrospun constructs: feasibility and safety investigation. *Urol J.* 2012;9(1):410-419.
 61. Alvarez-Perez MA, Guarino V, Cirillo V, Ambrosio L. Influence of gelatin cues in PCL electrospun membranes on nerve outgrowth. *Biomacromolecules.* 2010;11(9):2238-2246.
 62. Hiep NT, Lee B-T. Electro-spinning of PLGA/PCL blends for tissue engineering and their biocompatibility. *J Mater Sci Mater Med.* 2010;21(6):1969-1978.
 63. Chanda A, Adhikari J, Ghosh A, Chowdhury SR, Thomas S, Datta P, et al. Electrospun chitosan/polycaprolactone-hyaluronic acid bilayered scaffold for potential wound healing applications. *Int J Biol Macromol.* 2018;116:774-785.
 64. Sadeghi A, Moztarzadeh F, Mohandesi JA. Investigating the effect of chitosan on hydrophilicity and bioactivity of conductive electrospun composite scaffold for neural tissue engineering. *Int J Biol Macromol.* 2019;121:625-632.
 65. Venugopal J, Ma L, Yong T, Ramakrishna S. In vitro study of smooth muscle cells on polycaprolactone and collagen nanofibrous matrices. *Cell Biol Int.* 2005;29(10):861-867.
 66. Fukunishi T, Best CA, Sugiura T, Shoji T, Yi T, Udelsman B, et al. Tissue-engineered small diameter arterial vascular grafts from cell-free nanofiber PCL/chitosan scaffolds in a sheep model. *PLoS One.* 2016;11(7):e0158555.
 67. Zhou Z, Yan H, Liu Y, Xiao D, Li W, Wang Q, et al. Adipose-derived stem-cell-implanted poly (ϵ -caprolactone)/chitosan scaffold improves bladder regeneration in a rat model. *Regen Med.* 2018;13(3):331-342.
 68. Hanczar M, Moazen M, Day R. The Significance of Biomechanics and Scaffold Structure for Bladder Tissue Engineering. *Int J Mol Sci.* 2021;22(23):12657.
 69. Martins PA, Fonseca AMRM, Santos A, Santos L, Mascarenhas T, Jorge RM, et al. Uniaxial mechanical behavior of the human female bladder. *Int Urogynecol J.* 2011;22(8):991-995.